Figure S1. Hachisako et al.

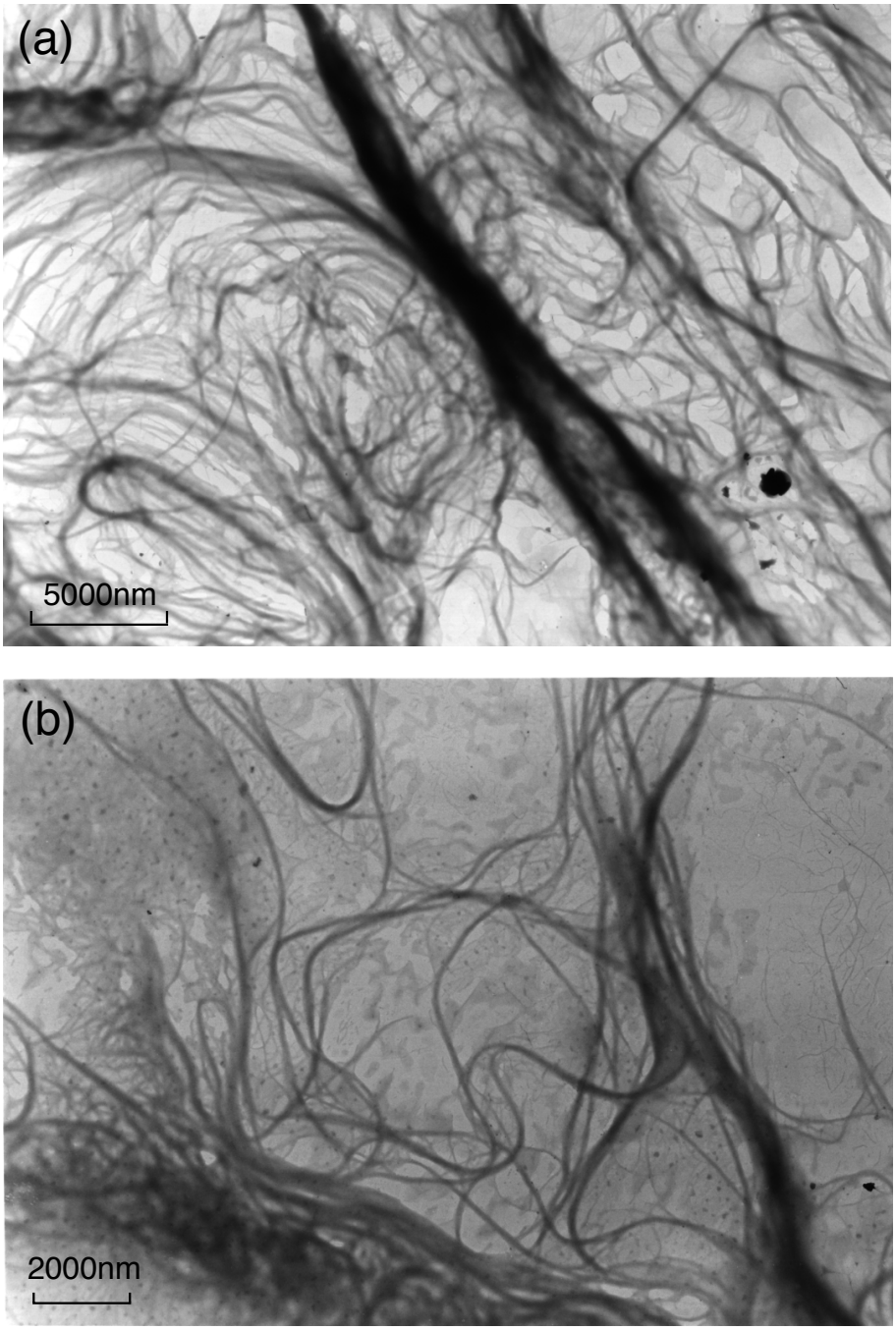

Figure S1. TEM images of xerogels obtained from organogels of (a) L-**1** and (b) L-**11** in chlorobenzene: post-stained with 2 wt% of aqueous ammonium molybdate: [L-**1**] = [L-**11**] = 1.0 mM.

Figure S2. Hachisako et al.

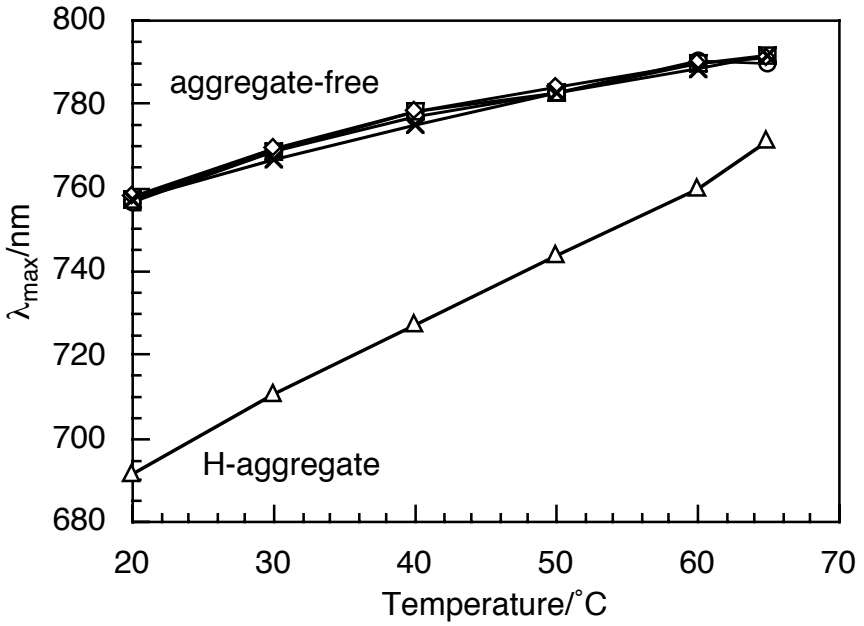

Figure S2. Concentration dependence of λ_{max} of E$_T$(30) in chlorobenzene:○; [E$_T$(30)] = 0.0325 mM,□; [E$_T$(30)] = 0.075 mM, ◇; [E$_T$(30)] = 0.15 mM,×; [E$_T$(30)] = 0.30 mM,△; [E$_T$(30)] ~ 1.5 mM (saturated solution).

Figure S3. Hachisako et al.

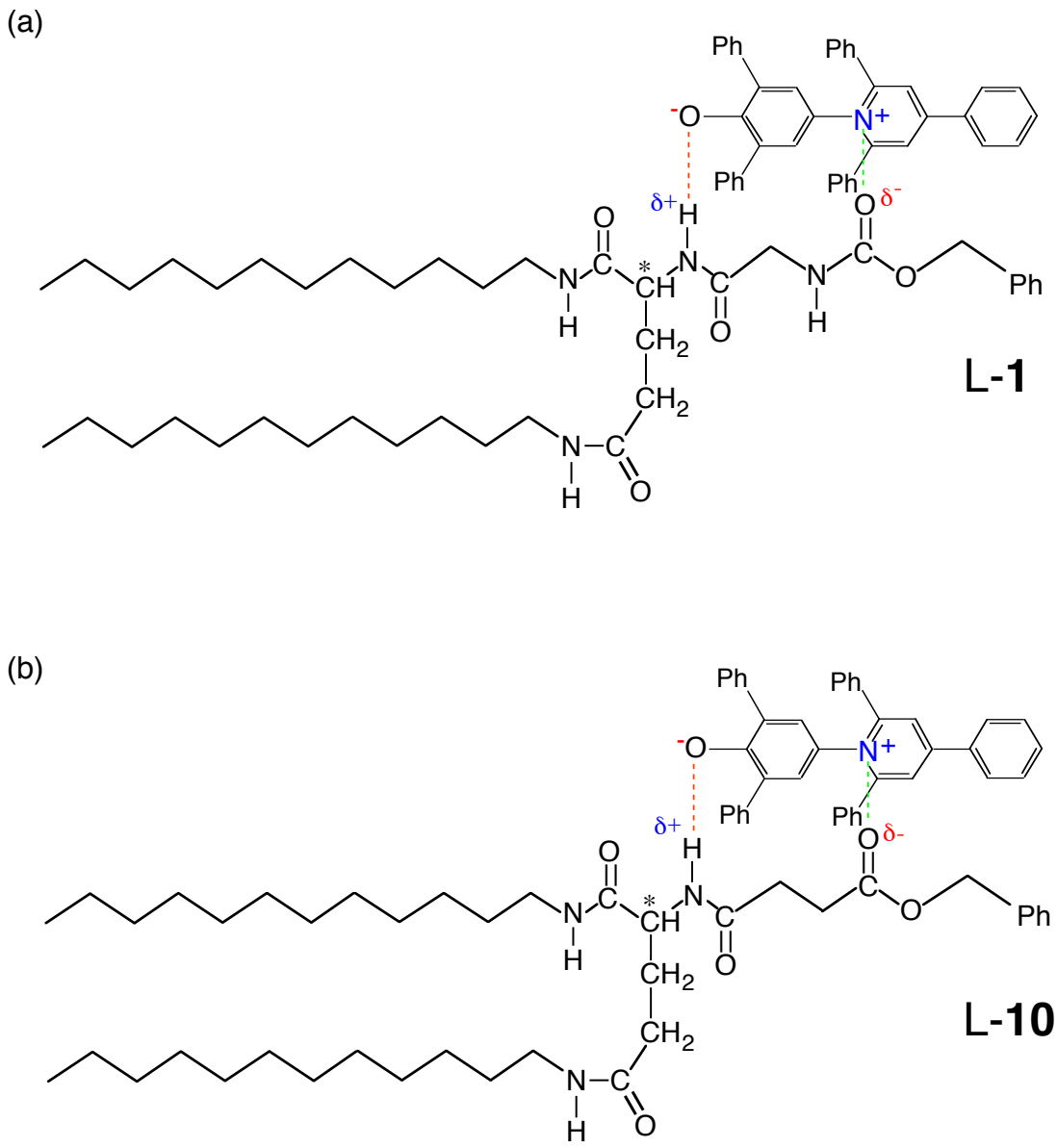

Figure S3. Schematic representation of intermolecular interactions between E$_T$(30) and lipids L-**1** (a) and L-**10** (b), respectively, in chlorobenzene.

Figure S4. Hachisako et al.

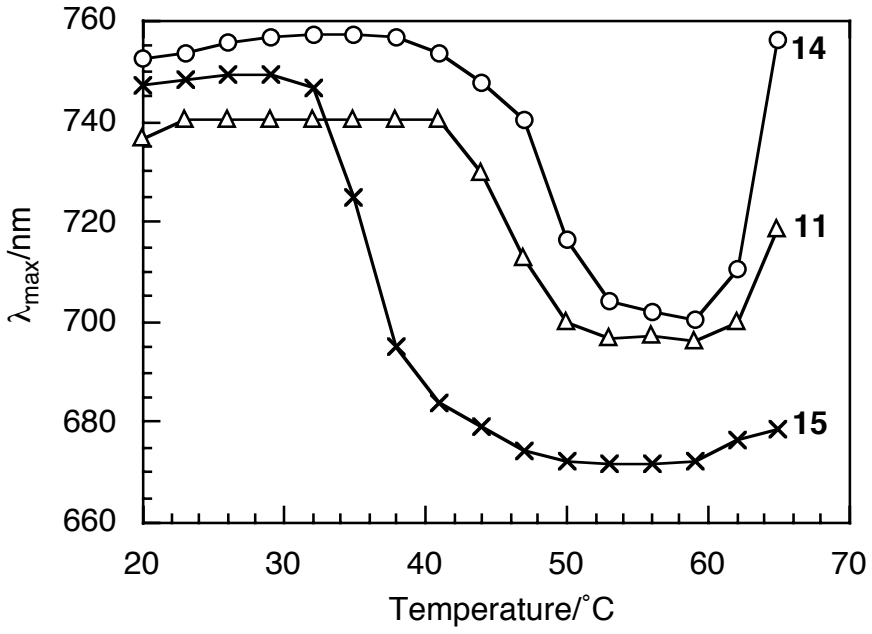

Figure S4. Temperature dependence of λ_{max} of $E_T(30)$ in the presence of lipid aggregates of L-**11**, L-**14**, and L-**15** in chlorobenzene.

Figure S5. Hachisako et al.

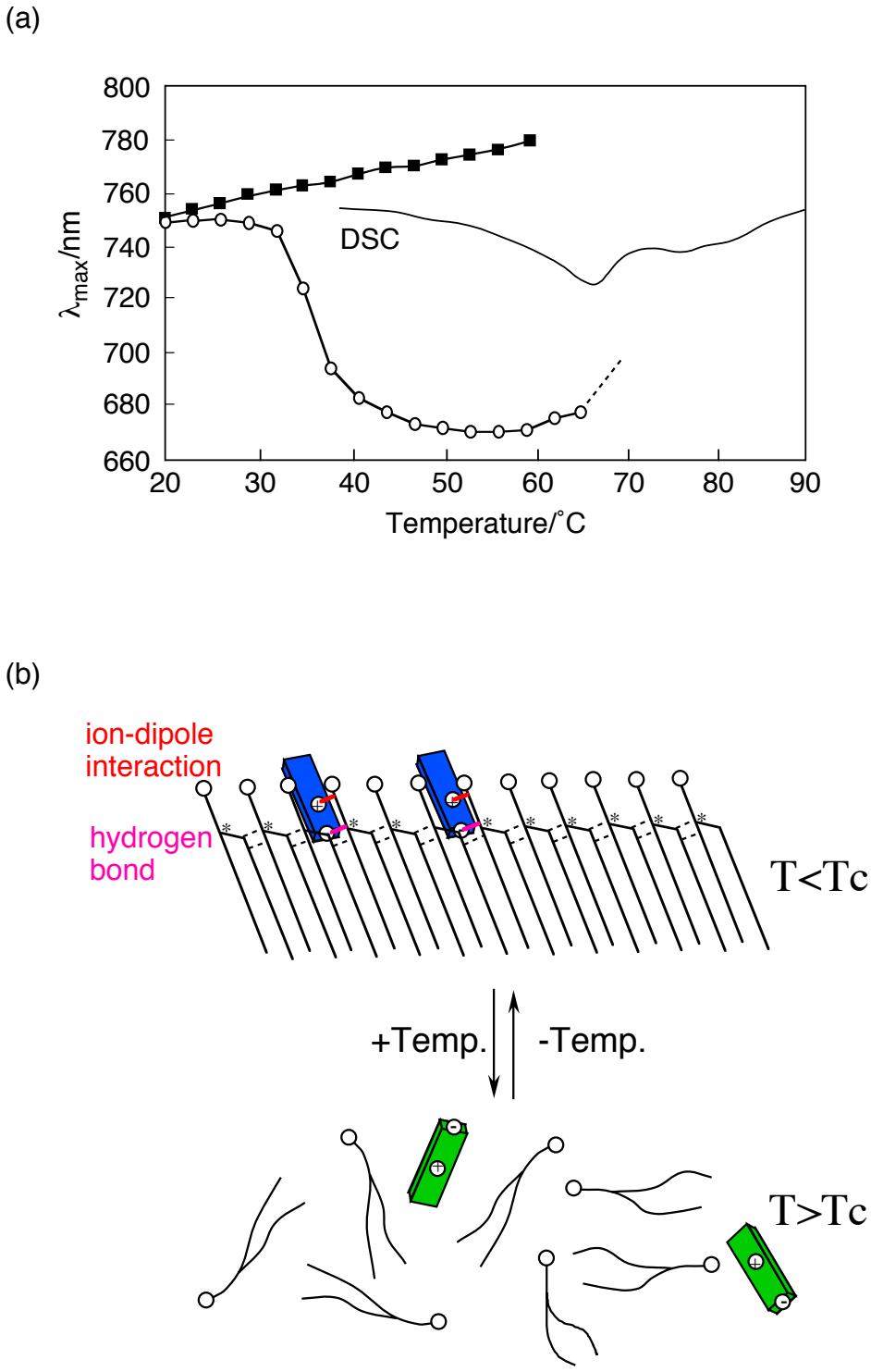

Figure S5. (a) Temperature dependence of λ_{max} of $E_T(30)$ (■) alone and (○) in the presence of lipid aggregates of L-**11** in chlorobenzene; (b) Schematic representation of interaction between lipid (L-**1**, L-**7**, L-**8**, L-**9**, L-**11**, DL-**11**, L-**14**, L-**15**, or L-**16**) and $E_T(30)$ in chlorobenzene. Bilayer structure is omitted for clarity.

Figure S6. Hachisako et al.

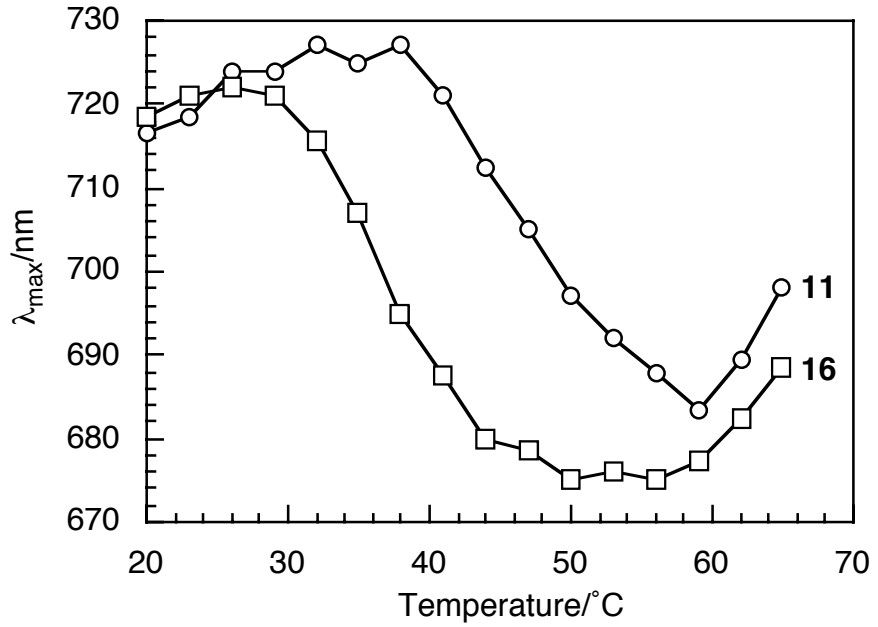

Figure S6. Temperature dependence of λ_{max} of $E_T(30)$ in the presence of lipids L-**11** and L-**16** in chlorobenzene: ○; L-**11**, □; L-**16**, [lipid] = 3.0 mM, [$E_T(30)$] = 0.15 mM, [lipid]/[$E_T(30)$] = 20.